APPLIED SCIENCES AND ENGINEERING

Minimizing friction, wear, and energy losses by eliminating contact charging

Khaydarali Sayfidinov[1], S. Doruk Cezan[2], Bilge Baytekin[1,2], H. Tarik Baytekin[1]*

One-fourth of the global energy losses result from friction and wear. Although friction and tribocharging were presented to be mutually related, reduction of friction and wear by eliminating tribocharges on common polymers, and decrease of power losses in devices with polymer parts were not shown to date. Here, we demonstrate that for common polymers, friction—which is strongly related to surface charge density—can be notably reduced by various methods of tribocharge mitigation, namely, corona discharging, solvent treatment, or placing a grounded conductor on the backside of one of the shearing materials. In our simple demonstrations, we found that by preventing tribocharge accumulation, a remarkable two-thirds of power loss during operation of simple mechanical devices with common polymers and plastic parts can be saved and wear can be reduced by a factor of 10. These demonstrations indicate important practical ramifications in mechanical systems with insulating parts.

INTRODUCTION

Since friction and wear are responsible for about a quarter of the total energy losses worldwide (*1*), new methods of minimizing these untoward effects could be of immense value for the energy-efficient economy of the future. One source of friction is the so-called contact electrification (also known as tribocharging) (*2*–*6*), whereby two insulating materials moving against each other develop net charges of opposite polarity and thus give rise to an attractive force between them. Although many previous studies (*7*–*12*) have considered the relation between tribocharging and friction, detailed microscopic understanding and its translation to the macroscopically observed energy losses and wear both remain elusive. Here, we consider various factors that influence both tribocharging and friction between macroscopic polymeric materials. We show that (i) the coefficient of dynamic friction [CoF(D)] is strongly dependent on the surface charge density and (ii) it can be significantly reduced by various methods of minimizing effective surface charges, namely, traditional corona discharging, solvent treatment, or placing a grounded conductor on the backside of one of the shearing materials. In particular, the last of these options is a very economical and technically straightforward means of minimizing attractive electrostatic forces between the shearing surfaces. We further demonstrate that elimination of surface charges by these simple means can save up to a remarkable two-thirds of power loss during operation of simple mechanical devices and can reduce wear by a factor of 10—both of these figures suggest practical ramifications of this work to various types of modern mechanical systems, many of which rely on insulating parts prone to charge accumulation.

Static and dynamic frictions depend on a multitude of chemical, physicochemical, physical, and mechanical properties of the contacting materials, as well as external conditions (*13*, *14*). Friction reflects various types of molecular interactions (*15*), phononic excitations (*11*), nature and reactivity of surface groups (*16*), crystallinity (*17*), surface roughness, and even scale (*18*) [e.g., negative friction in some nanoscale systems (*19*)]. Dry friction is quantified by coefficient of friction (CoF)—the ratio of the friction force to the normal load. However, CoF is not necessarily constant or steady over long periods, repeatable, or single valued (*20*), because friction arises from several mechanisms acting simultaneously at macro- to nanoscales (*21*). One of these mechanisms is the creation of surface charges upon contact and/or shearing of two different [or identical (*22*)] materials. Contact electrification is itself a topic of vibrant research, and it has only been in recent years that its fundamental aspects [creation of heterogeneous charge mosaics (*5*, *6*, *23*, *24*), importance of material transfer (*25*), and creation of both charges and radicals (*26*, *27*)] have been elucidated. Despite these recent advances in understanding the mechanism of tribocharging, literature data on the direct relation between friction and tribocharging are surprisingly sparse (*28*). Nevertheless, earlier studies on metal/polymer contacts [e.g., sliding a millimeter-sized gold ball on polymethylmethacrylate (PMMA) (*7*)], ceramic/polymer contacts [e.g., alumina-polytetrafluoroethylene (PTFE) sliding contact in the presence of a lubricant (*8*)], and polymer/polymer contacts (*9*) showed existence of cross-relation between tribocharge and friction. Another recent report, in which a metal pin slides on the PTFE surface, confirmed unequivocally that triboelectricity and friction have the same origin (*10*). At the nanoscale, tribocharging and subsequent charge transfer from an insulating monolayer to an atomic force microscopy tip results in large electrostatic frictional forces (*11*). However, to our knowledge, the contribution of tribocharging to friction-induced wear and energy losses at polymer/polymer contacts, and minimization of friction by tribocharge reduction (as we discuss here), has not yet been reported.

RESULTS AND DISCUSSION

Figure 1A illustrates that the contribution from tribocharging is quite substantial, especially for machines with insulator parts; a simple rotor with polymer blades running on another polymer surface can heat up or even stop operating because of increasing friction through increased charging and electrostatic adhesion between the two surfaces. In sharp contrast, when the charges are removed by using a corona discharge gun, the local heating and energy dissipation are reduced, and the energy consumption is lowered by ca. 66% (Fig. 1B).

[1]UNAM-National Nanotechnology Research Center, Bilkent University, 06800 Ankara, Turkey. [2]Chemistry Department, Bilkent University, 06800 Ankara, Turkey.
*Corresponding author. Email: baytekin@unam.bilkent.edu.tr

To quantify contact charging, concomitant friction, and the power savings expected upon charge removal, we used a "textbook" setup in which a solid cylinder-shaped object is placed at the top of an inclined plane and allowed to slide freely toward the bottom, after which time the body is moved back to the starting position and more sliding cycles are repeated. A cylindrical wood piece with a polyethylene terephthalate (PET) film base slides on cellulose (as shown in Fig. 2A; see also movie S2), in the process acquiring tribocharges quantified in Fig. 2B for different numbers of sliding cycles (see the Supplementary Materials for details on charge measurements). Both the magnitude of charges and the sliding times increase from run to run, on the 19th downhill slide, and the sliding time quadruples compared to the first run. In a related demonstration, to illustrate the increase in the coefficient of friction [CoF(S); equal to tan θ], the angle of inclination at which sliding commences also increases with consecutive runs (Fig. 2C). However, when the tribocharges on the sliding surfaces are eliminated by a Zerostat corona discharge gun, both the sliding time and the "θ offset" revert to their original values during the first sliding (Fig. 2, B and C).

With these illustrative examples, we then used a friction tester (Hanatek Advanced Friction Tester) to record the CoF(S) and CoF(D) of pairs of various commonly used polymers (see the Supplementary Materials for further experimental details) for repeated horizontal sliding cycles. Charges on the sliding pieces were also recorded after each run. As we expected, both tribocharge density and CoF(D) increased during consecutive runs (Fig. 3A), with the mutual relationship between these quantities quantified in figs. S1 and S2. We note that the degree of material transfer between the two sliding surfaces accompanying tribocharging (*25*) may also affect the measured CoF(D) (fig. S3). Next, we tested various methods of dissipating the tribocharges developed, namely, rinsing the contacting surfaces with a solvent, corona discharge, or covering the backside of one or both materials with a layer of a conductive material grounded through a wire (Fig. 3). For all these approaches and for all the discharged polymer pairs, friction did not significantly increase upon repeated sliding runs. Data for a representative PTFE sliding on cellulose are shown in Fig. 3 (C to E). Upon grounding with a metal backing (Fig. 3D, red dots), the CoF(D) during the 35th sliding cycle was only 9% higher than during the first run (Fig. 3E, red dots), compared to a more than 50% increase when the polymer is not grounded (Fig. 3E, black dots). We note here that, for practical uses, grounding might be the most economical and technically straightforward method; however, we found that the corona discharge method is the best method to keep friction coefficients at a minimum, and that the ethanol-rinsing method is the best method to prevent wear, presumably because this method also removes the debris formed during sliding (fig. S4). Notably, although there is no substantial change in the crystallinity of polymers (fig. S5) with or without tribocharge removal, we detected a decrease in the extent tribochemical changes (e.g., oxidation and fluorination) with continuous removal of tribocharges upon sliding, in comparison to the cases where the charges were allowed to accumulate on the polymer surfaces (fig. S6).

So far, we showed some of the direct friction control methods via tribocharge dissipation. Tribocharging (and hence friction) can also be controlled by manipulating external factors such as atmosphere and humidity (*29*–*31*). We briefly show the effect of these external factors on tribocharging and friction in figs. S7 and S8. We also show the effect of net charge polarity (*32*) on the CoF(D) in a separate set of experiments (figs. S9 and S10).

As we stated before, the most important corollaries of this work are in the different types of mechanical systems with insulating parts. To provide a simple demonstration of reducing friction in such a system, we monitored the rotation of a ball bearing with a plastic ring and glass balls with and without a continuous discharging, as shown in Fig. 4A. Without any discharging, at 200 rpm, resistance of the ring against rotation, which is measured by an attached load cell, increases with rotation time (Fig. 4B; for details, see fig. S11). We showed that even a single "shot" of a corona discharge gun instantly decreases the friction force from 0.0125 to 0.0060 N upon continuous operation of the bearing (Fig. 4B).

Friction-initiated wear in polymeric contacts can also be reduced by the elimination of contact charges: If the acquired charge density on a thick (0.5 cm) piece of polyvinylchloride (PVC; 2.5 cm × 2.5 cm) that repeatedly slid on cellulose (20 cm × 25 cm, θ = 20°) is kept below −0.2 nC/cm^2 by continuous corona discharging of the sliding plane, after 35 runs the wear at the PVC surface is

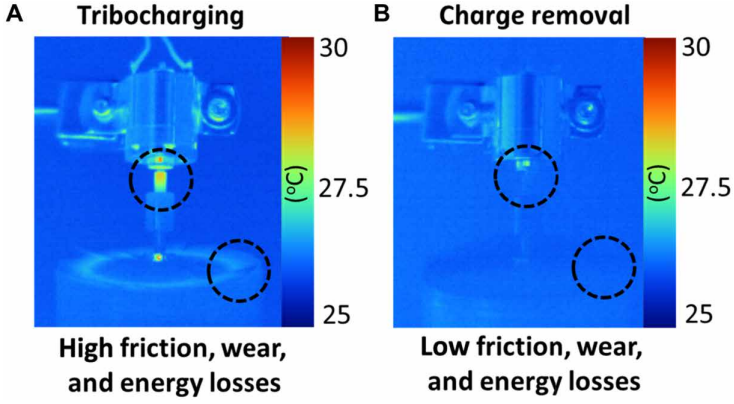

Fig. 1. Thermal camera images of an operating motor with insulating parts demonstrating a decrease in heat dissipation upon continuous removal of tribocharges, which implies lower friction, wear, and energy consumption. Polysulfone (PSU) polymer blades are mounted on a shaft of a DC electric motor and are sweeping against another polymer surface (shown here, cellulose). (**A**) Tribocharging causes high electrostatic adhesion, leading to high friction, wear, and energy consumption, as imaged in the temperature increase at the motor's shaft and polymer blades upon operation (black circles). (**B**) The same rotor system does not heat up, shows lower rates of wear, and consumes lower power [about one-third of the system in (A)] when charges are continuously being removed (see movie S1, Supplementary Text, and Fig. 4H for details on calculation of the energy consumption).

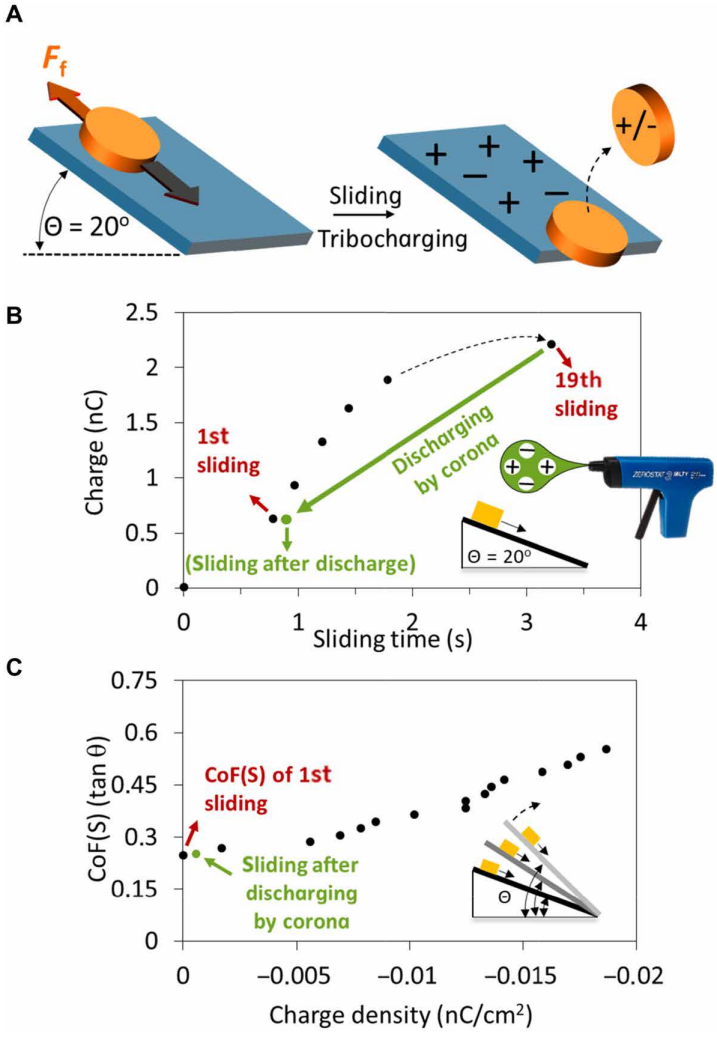

Fig. 2. Friction and tribocharges increase upon repeated "runs" of a polymer sliding on an inclined plane. (**A**) Sliding of pucks (with polymer sheet bases) on cellulose (on inclined plane) causes tribocharging of the surfaces and leads to an increase in friction. (**B**) Sliding time of the puck and charge acquired on the base both increase with repeated sliding runs. When the sliding surfaces are discharged by a Zerostat corona discharge gun, the sliding time resets back to the value in the first sliding (green arrow) [puck = wood (2 cm diameter); polymer sheet = PET (2 cm diameter, 0.20 mm thick); θ = 20°] (**C**) θ, in which the sliding can be initiated on the inclined plane at the repeated cycles, increasing with tribocharging at repeated cycles; again, reset is possible by corona discharging [puck = wood (2 cm diameter); polymer sheet = PTFE (1.5 cm diameter, 3.0 mm thick); relative humidity = 22%; see movie S2 and the Supplementary Materials for further experimental details].

reduced [10 wear lines in polarized optical microscopy (POM) image] in comparison to the case in which the same piece is allowed to slide for 35 runs without any discharge (ca. 100 wear lines on the same area) (Fig. 4, C to F).

Last, to show how the removal of tribocharges may eventually minimize the friction-related energy consumption in a device, we constructed a simple yet illustrative system: We attached 0.2-mm-thick PSU blades on the shaft of a DC electric motor (see the Supplementary Materials for further experimental details). When PSU blades are allowed to come into contact with a flat cellulose surface, this contact and rotational sliding quickly generates tribocharges on both polymer surfaces (Fig. 4G and movie S1). During normal operation (in which the charges are allowed to accumulate on PSU blades and on the cellulose surface), the current drawn by the DC electric motor increases (in this example shown in movie S1, from 83 to 220 mA), the motor consumes about 440 mW, and, because of the increased tribocharges and friction between the surfaces, the rotation stops (Fig. 4H). At this point, if the contacting surfaces were corona discharged, then the operation resumes with lower energy consumption (83 mA, 166 mW, about one-third of the value measured for "tribocharged" motor system). The minimized friction and energy consumption can also be visualized by thermal images of the motor working under continuous discharging (Fig. 4, I and J).

CONCLUSION

From our results, we conclude that continuous discharging might be used to reduce friction, wear, and energy consumption in systems with moving insulator parts. Engineering the simple systems and their results displayed in this report might be beneficial for many current industries using polymer and cellulosic (*33*) materials. The

concept displayed here would also be important for emerging devices, e.g., intricate micro- and nanoelectromechanical systems, because surface forces become extremely prominent at small dimensions.

MATERIALS AND METHODS

Materials

Pure cellulose sheets (165 μm; Southworth Resume Paper, 100% cotton) were used as a stationary material, which were laid on the nonmagnetic metal platform of the friction tester. A new sheet was used for each of the polymers, except for consecutive sliding experiments. Flat polymer sheets (5 cm × 5 cm) with a thickness of less than 500 μm [PVC, PTFE, polyvinylidene difluoride, polypropylene (charging negatively against cellulose), polycarbonate, PMMA, PSU, polyimide-Kapton, and polyester polyethylene glycol (charging positively against cellulose)] were attached to the bottom of a flat, 2-mm-thick, 0.6-g insulating wood piece, and polymer-wood assemblies were presented as sliding objects.

Friction measurements

A fully automated and computer-controlled friction tester (Hanatek Advanced Friction Tester) was used for the friction experiments to obtain friction versus distance data as well as static and dynamic friction coefficients with high accuracy. Polymer sheet-wood assemblies were attached directly to the load cell. Normal load was changed by putting round metal pieces (brass) with different weights at the top of the wooden support when necessary. The sliding speed was set to 1200 mm/min for all the experiments. Weights were grounded before the charge measurements. A homemade metal frame polymer chamber was used in the sliding experiments that were performed in air or under continuous flow of nitrogen and argon.

Surface tribocharge and surface potential measurements

The tribocharge on the surface polymers (5 cm × 5 cm) was measured after each sliding experiment using a homemade Faraday cup that is connected to an electrometer (Keithley Instruments model 6514). Data acquisition was performed with LabVIEW code, and tribocharge densities were reported in nC/cm^2. During measurements, an antistatic wristband was used to ground the sample holding tweezers. Surface potential measurements were done using an electrostatic voltmeter (TREK model 370), with a macroscopic Kelvin probe (3800E-2 end view) attached.

Humidity measurements

Humidity and temperature were recorded using a hygrometer (Traceable 37950-11, Cole-Parmer).

Surface analysis

X-ray photoelectron spectroscopy (XPS) measurements were performed using a spectrometer (Thermo Fisher Scientific, Waltham,

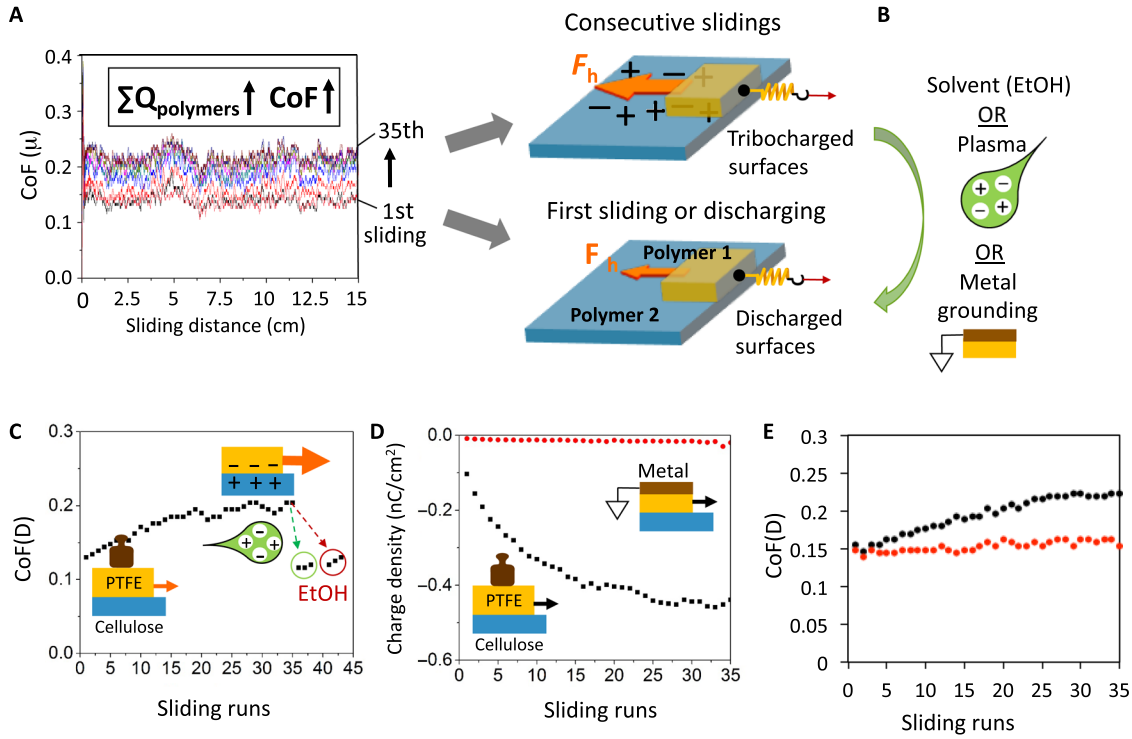

Fig. 3. Various methods of tribocharge removal on sliding polymer surfaces can control friction between them. Sliding a PTFE piece horizontally on cellulose, (**A**) friction between PTFE and cellulose increases with sliding distance and consecutive runs, as measured by the Hanatek Advanced Friction Tester. (**B**) Removal of tribocharges by various methods of charge dissipation. (**C**) Reset of CoF(D) to its initial value with corona discharge treatment (data marked with green circle) and ethanol rinsing (data marked with red circle) of PTFE on cellulose at the 35th run (sliding distance per run = 15 cm). (**D**) Attaching a grounded metal (flat brass, 0.25 mm thick) to the back of the PTFE piece prevents both the accumulation of charges at the polymer surface and (**E**) the increase in the CoF(D) (red dots = metal-grounded PTFE on cellulose; black dots = PTFE on cellulose). PTFE, 5 cm × 5 cm × 0.25 mm; cellulose, 10 cm × 20 cm × 0.165 mm; F_N = 0.15 N is adjusted by putting additional weight on bare PTFE or metal backing on PTFE (see the Supplementary Materials and figs. S1, S2, and S7 to S10 for further experimental details and the effects of sign of net charge, contact area, load, material transfer between the surfaces, and atmosphere on simultaneous tribocharging and friction).

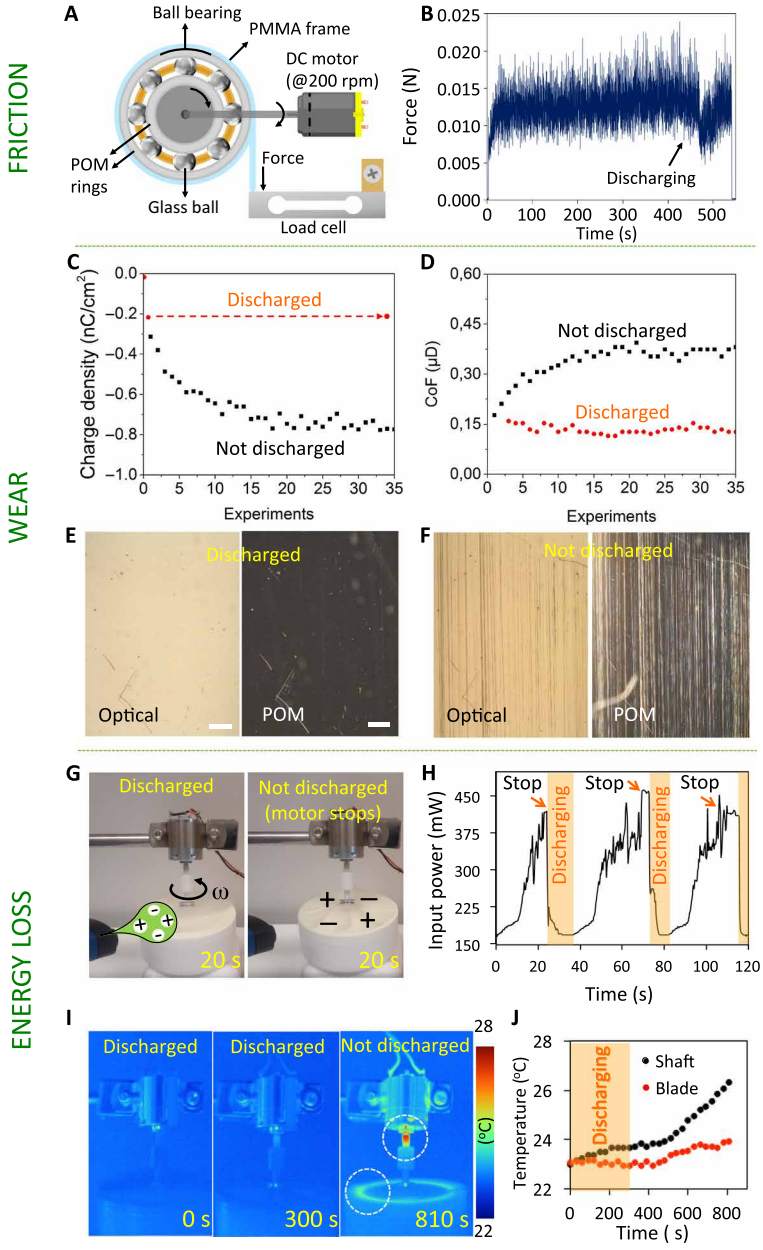

Fig. 4. Friction, wear, and power losses can all be minimized in some common mechanical systems with insulator contacts. FRICTION: (**A**) On a ball bearing with inner and outer polyoxymethylene polymer rings (diameters, 52 and 25 mm) and nine glass balls rotated at 200 rpm (see the Supplementary Materials for details of the experiment), (**B**) resistance increases with rotation time; however, even a single shot of corona discharge gun can reduce this force from 0.0125 to 0.0075 N. WEAR: During consecutive runs of PVC pieces (2.5 cm × 2.5 cm × 0.25 mm) on an inclined plane (cellulose: 20 cm × 25 cm, θ = 20°), (**C**) with continuous corona discharge of the sliding plane (red dots), (**D**) one can keep the CoF(D) of the sliding PVC piece (2.5 cm × 2.5 cm × 0.25 mm) at a minimal value for 35 runs. (C and D) For comparison, black dots show the control experiment (not discharged system). (**E**) The "discharged" piece in (C) has only a slight wear (10 macro-wear lines on POM image) after 35 runs, whereas (**F**) the "not discharged" piece had ca. 100 wear lines after the same number runs (F_N = 0.15 N). Scale bars, 200 μm. POWER LOSS: (**G**) Rotating PSU blades attached to a 12-V DC electric motor (Mabuchi RS 555, operated at 2 V) are triboelectrified upon sweeping against a cellulose sheet (left); after ca. 20 s, the blades stop due to highly increased electrostatic adhesion and friction between the blades and the sheet (right) (see movie S1). (**H**) Change in the input power of the DC electric motor used in (G). The motor stops by itself after acquiring tribocharges (ca. 20 s; at this point, electrostatic potential on polymer blades = +2500 V, cellulose = −2500 V); however, it can be restarted by corona discharging, which minimizes the input power. (**I**) Left to right: Infrared images of the motor in (G) upon operation with continuous discharging between 0 and 300 s. After 300 s, the motor is not discharged anymore and the temperature at the shaft and blades rises quickly, as shown in (**J**). For details on calculating the recovered power loss, see Supplementary Text.

MA) with a monochromatized Al K-Alpha X-ray source; the spot size is set to 400 μm. For scanning electron microscopy imaging, the FEI Quanta 200F ESEM was used. The beam accelerating voltage was set to 5 kV. For energy-dispersive x-ray (EDX) measurements, samples were coated with ~10 nm of Au/Pd alloy before EDX analysis; an accelerating voltage of 15 kV was used during imaging.

X-ray diffraction

X-ray diffraction (XRD) measurements were performed using a PANalytical X'Pert PRO x-ray diffractometer with Cu Kα radiation.

SUPPLEMENTARY MATERIALS

Supplementary material for this article is available at http://advances.sciencemag.org/cgi/content/full/4/11/eaau3808/DC1

Supplementary Text

Fig. S1. Dynamic and static coefficients of friction versus normal load for the PTFE-cellulose system.

Fig. S2. Size versus charge and size versus CoF; load versus charge compared with load versus CoF for sliding polymer pairs.

Fig. S3. Spectroscopic evidence for material transfer upon polymer sliding.

Fig. S4. Comparison of various methods of tribocharge removal on sliding polymer surfaces: friction, charge, and wear reduction.

Fig. S5. XRD analyses of sliding surfaces with and without elimination of tribocharges.

Fig. S6. HIRES-XPS analyses of the cellulose surface with and without elimination of tribocharges during PTFE sliding.

Fig. S7. Friction and tribocharging for PVC sliding on cellulose in various atmospheres.

Fig. S8. Friction and tribocharging for PVC sliding on cellulose in various atmospheres and relative humidity values.

Fig. S9. The relation between friction and tribocharging for negatively charged polymers sliding on cellulose for the consecutive sliding experiments.

Fig. S10. The relation between friction and tribocharging for positively charged polymers sliding on cellulose for the consecutive sliding experiments.

Fig. S11. Friction reduction in a bearing with insulator parts.

Movie S1. Increase in electrical energy consumption of a DC motor with polymer blades.

Movie S2. Friction and tribocharges increase upon repeated sliding runs of a polymer sliding on an inclined plane.

References (*34*–*44*)

REFERENCES AND NOTES

1. K. Holmberg, A. Erdemir, Influence of tribology on global energy consumption, costs and emissions. *Friction* **5**, 263–284 (2017).
2. R. G. Horn, D. T. Smith, Contact electrification and adhesion between dissimilar materials. *Science* **256**, 362–364 (1992).
3. W. R. Harper, *Contact and Frictional Electrification* (Oxford Univ. Press, 1967).
4. M. W. Williams, Triboelectric charging of insulating polymers—Some new perspectives. *AIP Adv.* **2**, 010701 (2012).
5. H. T. Baytekin, A. Z. Patashinski, M. Branicki, B. Baytekin, S. Soh, B. A. Grzybowski, The mosaic of surface charge in contact electrification. *Science* **333**, 308–312 (2011).
6. U. G. Musa, S. D. Cezan, B. Baytekin, H. T. Baytekin, The charging events in contact-separation electrification. *Sci. Rep.* **8**, 2472 (2018).
7. R. Budakian, S. J. Putterman, Correlation between charge transfer and stick-slip friction at a metal-insulator interface. *Phys. Rev. Lett.* **85**, 1000–1003 (2000).
8. H. Wistuba, A phenomenon of triboelectrization in aluminium oxide–polytetrafluoroethylene sliding contact joint operating under reduced lubrication conditions. *Wear* **208**, 118–124 (1997).
9. T. A. L. Burgo, C. A. Silva, L. B. S. Balestrin, F. Galembeck, Friction coefficient dependence on electrostatic tribocharging. *Sci. Rep.* **3**, 2384 (2013).
10. T. A. L. Burgo, A. Erdemir, Bipolar tribocharging signal during friction force fluctuations at metal-insulator interfaces. *Angew. Chem. Int. Ed.* **126**, 12297–12301 (2014).
11. J. Krim, Friction and energy dissipation mechanisms in adsorbed molecules and molecularly thin films. *Adv. Phys.* **61**, 155–323 (2012).
12. K. Nakayama, Tribocharging and friction in insulators in ambient air. *Wear* **194**, 185–189 (1996).
13. G. He, M. H. Müser, M. O. Robbins, Adsorbed layers and the origin of static friction. *Science* **284**, 1650–1652 (1999).
14. A. Abdelbary, *Wear of Polymers and Composites* (Elsevier, 2014).
15. M. Lekka, A. J. Kulik, S. Jeney, J. Raczkowska, J. Lekki, A. Budkowski, L. Forró, Friction force microscopy as an alternative method to probe molecular interactions. *J. Chem. Phys.* **123**, 014702 (2005).
16. F. Galembeck, T. A. L. Burgo, L. B. S. Balestrin, R. F. Gouveia, C. A. Silva, A. Galembeck, Friction, tribochemistry and triboelectricity: Recent progress and perspectives. *RSC Adv.* **4**, 64280–64298 (2014).
17. S. K. Biswas, K. Vijayan, Friction and wear of PTFE—A review. *Wear* **158**, 193–211 (1992).
18. Z. Ye, A. Martini, Atomistic simulation of the load dependence of nanoscale friction on suspended and supported graphene. *Langmuir* **30**, 14707–14711 (2014).
19. Z. Deng, A. Smolyanitsky, Q. Li, X.-Q. Feng, R. J. Cannara, Adhesion-dependent negative friction coefficient on chemically modified graphite at the nanoscale. *Nat. Mater.* **11**, 1032–1037 (2012).
20. K. C. Ludema, *Friction, Wear, Lubrication: A Textbook in Tribology* (CRC Press, 2000).
21. M. Nosonovsky, B. Bhushan, *Multiscale Dissipative Mechanisms and Hierarchical Surfaces: Friction, Superhydrophobicity, and Biomimetics* (Springer-Verlag, 2008).
22. M. M. Apodaca, P. J. Wesson, K. J. M. Bishop, M. A. Ratner, B. A. Grzybowski, Contact electrification between identical materials. *Angew. Chem. Int. Ed.* **49**, 946–949 (2010).
23. T. Shinbrot, T. S. Komatsu, Q. Zhao, Spontaneous tribocharging of similar materials. *Europhys. Lett.* **83**, 24004 (2008).
24. T. A. L. Burgo, T. R. D. Ducati, K. R. Francisco, K. J. Clinckspoor, F. Galembeck, S. E. Galembeck, Triboelectricity: Macroscopic charge patterns formed by self-arraying ions on polymer surfaces. *Langmuir* **28**, 7407–7416 (2012).
25. H. T. Baytekin, B. Baytekin, J. T. Incorvati, B. A. Grzybowski, Material transfer and polarity reversal in contact charging. *Angew. Chem. Int. Ed.* **51**, 4843–4847 (2012).
26. B. Baytekin, H. T. Baytekin, B. A. Grzybowski, What really drives chemical reactions on contact charged surfaces? *J. Am. Chem. Soc.* **134**, 7223–7226 (2012).
27. H. T. Baytekin, B. Baytekin, T. M. Hermans, B. Kowalczyk, B. A. Grzybowski, Control of surface charges by radicals as a principle of antistatic polymers protecting electronic circuitry. *Science* **341**, 1368–1371 (2013).
28. F. P. Bowden, D. Tabor, *Friction: Introduction to Tribology* (Heinemann Educational Publishers, 1974).
29. K. Hosotani, K. Hiratsuka, Effects of friction type and humidity on triboelectrification and triboluminescence among eight kinds of polymers. *Tribol. Int.* **55**, 87–99 (2012).
30. E. Németh, V. Albrecht, G. Schubert, F. Simon, Polymer tribo-electric charging: Dependence on thermodynamic surface properties and relative humidity. *J. Electrostat.* **58**, 3–16 (2003).
31. H. T. Baytekin, B. Baytekin, S. Soh, B. A. Grzybowski, Is water necessary for contact electrification? *Angew. Chem. Int. Ed.* **50**, 6766–6770 (2011).
32. D. J. Lacks, R. M. Sankaran, Contact electrification of insulating materials. *J. Phys. D Appl. Phys.* **44**, 453001 (2011).
33. K. Holmberg, R. Siilasto, T. Laitinen, P. Andersson, A. Jäsberg, Global energy consumption due to friction in paper machines. *Tribol. Int.* **62**, 58–77 (2013).
34. M. M. Shahin, Mass-spectrometric studies of corona discharges in air at atmospheric pressures. *J. Chem. Phys.* **45**, 2600–2605 (2004).
35. L. S. McCarty, A. Winkleman, G. M. Whitesides, Ionic electrets: Electrostatic charging of surfaces by transferring mobile ions upon contact. *J. Am. Chem. Soc.* **129**, 4075–4088 (2007).
36. V. Nguyen, R. Yang, Effect of humidity and pressure on the triboelectric nanogenerator. *Nano Energy* **2**, 604–608 (2013).
37. N. Tas, T. Sonnenberg, H. Jansen, R. Legtenberg, M. Elwenspoek, Stiction in surface micromachining. *J. Micromech. Microeng.* **6**, 385–397 (1996).
38. K. R. Makinson, D. Tabor, Friction and transfer of polytetrafluoroethylene. *Nature* **201**, 464–466 (1964).
39. J. Lowell, The role of material transfer in contact electrification. *J. Phys. D Appl. Phys.* **10**, L233 (1977).
40. W. R. Salaneck, A. Paton, D. T. Clark, Double mass transfer during polymer-polymer contacts. *J. Appl. Phys.* **47**, 144 (2008).
41. Y. Sun, X. Huang, S. Soh, Solid-to-liquid charge transfer for generating droplets with tunable charge. *Angew. Chem. Int. Ed.* **55**, 9956–9960 (2016).
42. A. E. Wang, P. S. Gil, M. Holonga, Z. Yavuz, H. T. Baytekin, R. M. Sankaran, D. J. Lacks, Dependence of triboelectric charging behavior on material microstructure. *Phys. Rev. Mater.* **1**, 035605 (2017).
43. J. K. Lancaster, Estimation of the PV relationships for thermoplastic bearing materials. *Tribology* **4**, 82–86 (1971).
44. F. E. Kennedy, Frictional heating and contact temperatures, in *Modern Tribology Handbook*, B. Bhushan, Ed. (CRC Press, 2000).

Acknowledgments: We thank Z. Yavuz for help in XRD measurements. **Funding:** This work was supported by the Scientific and Technological Research Council of Turkey (TÜBİTAK) under project number 214M358. H.T.B. acknowledges a Marie Sklodowska-Curie fellowship with project number H2020-MSCA-IF-2015_707643. B.B. acknowledges TÜBA GEBIP 2017 award. **Author contributions:** H.T.B. conceived the idea. B.B. and H.T.B. designed and directed the experiments. K.S. and S.D.C. carried out the experiments and contributed equally. B.B. and H.T.B. wrote the manuscript with contributions from all co-authors. **Competing interests:** The authors declare that they have no competing interests. **Data and materials availability:** All data needed to evaluate the conclusions in the paper are present in the paper and/or the Supplementary Materials. Additional data related to this paper may be requested from the authors.

Submitted 5 June 2018
Accepted 16 October 2018
Published 16 November 2018
10.1126/sciadv.aau3808

Citation: K. Sayfidinov, S. D. Cezan, B. Baytekin, H. T. Baytekin, Minimizing friction, wear, and energy losses by eliminating contact charging. *Sci. Adv.* **4**, eaau3808 (2018).

Minimizing friction, wear, and energy losses by eliminating contact charging

Khaydarali Sayfidinov, S. Doruk Cezan, Bilge Baytekin and H. Tarik Baytekin

Sci Adv **4** (11), eaau3808.
DOI: 10.1126/sciadv.aau3808